Progress in Physics of Applied Materials 1 (2021) 44 – 49

Semnan University

Progress in Physics of Applied Materials

journal homepage: https://ppam.semnan.ac.ir/

Numerical study of influences of the input current frequency on the induction heating process

M. H. Tavakoli*, H. Karbaschi

Physics Department, Bu-Ali Sina University, Hamedan 65174, I.R. Iran

ARTICLE INFO

Article history:
Received: 16 June 2021
Revised: 28 August 2021
Accepted: 11 September 2021

Keywords:
Induction heating
Finite element analysis
Modeling
Metals

ABSTRACT

In this article, the effect of input current frequency on the induction heating process was investigated using a numerical method. We used a 2D finite element method (FlexPDE package) to solve the governing equations in combination with the boundary conditions. The obtained computational results show that this parameter has a great effect on the spatial distribution and the amount of heat produced in different parts of the induction heating system. For all workpiece thicknesses, the amount of heat generated in the workpiece and the RF coil decreases with increasing frequency. Also, changes in driving frequency can shift the location of the maximum point of energy production along the outer surface of the workpiece sidewall. In low frequencies, the maximum amount of heat is located at the middle portions of the outer surface of the workpiece wall, and by frequency increasing, it is shifted toward the two corners of the workpiece surface. These results will help us to select a proper frequency range for different applications of induction heating during material processing.

1. Introduction

Induction heating is one of the most popular processes for heating electrically conductive materials (usually a metal) by electromagnetic induction. Induction heating has many advantages such as fast heating, high production rates, ease of automation and control, and safe and clean working. This process has many applications in material processing, such as heat treating, joining, welding, brazing, soldering, melting, and crystal growth. An induction heating installation has three important parts: a source of high-frequency alternating current, an induction coil (RF-coil), and a workpiece (metallic material) to be heated.

In the induction heating process, an induction coil surrounds the workpiece and an alternating electric current passes through it. This current creates time-varying electromagnetic fields in the environment (Ampere and Faraday law). These fields penetrate the metal parts of the system, such as the workpiece and the induction coil. The penetration depth depends on the electrical conductivity, the relative magnetic permeability, and the frequency of the input current. As a result, eddy currents will be produced in the workpiece and other metallic parts where the electrical resistance leads to Joule heating (I^2R) of the material in the form of temporal and spatial volumetric heating.

Today, more and more induction heating designers are shifting their development process from traditional empirical methods (trial and error) to computer simulation or a combination of both procedures. Computer simulation provides a lot of information about system dynamics for induction process designers. It can also be used to explain, demonstrate and predict process sensitivity to any change in an induction system [1–5].

The spatial distribution and amount of induced heat in the workpiece and induction coil are the major parameters to be determined. Understanding the physics of these properties is quite crucial and important when designing induction heating systems. The selection of the correct frequency for any application is one of the key elements of any successful system and has a great influence on the amount of generated energy.

In this article, a two-dimensional axial symmetry steady-state mathematical model of the induction heating process has been applied to investigate the influences of the input current frequency on the induced eddy currents, volumetric generated heat as well as coil efficiency in the system.

2. Mathematical model

2.1. The basic equations

The mathematical model used for our numerical calculation has been described in detail elsewhere [6]. It can be summarized as follow. The assumptions are: (1) the heating system is axis-symmetric, (2) all materials are

* Corresponding author. Tel.: +989183180323
E-mail address: mhtvkl@gmail.com

DOI: 10.22075/PPAM.2021.23704.1009

isotropic, non-magnetic and have no net electric charge, (3) the displacement current is neglected, (4) the distribution of driving electrical current (also voltage) in the RF-coil is uniform, (5) the currents (impressed and induced) have a steady-state quality and as a result, the electromagnetic field quantities are harmonically oscillating functions with a single frequency. Under these assumptions, the governing equations are;

$$\frac{\partial}{\partial r}\left(\frac{1}{r}\frac{\partial WB}{\partial r}\right) + \frac{\partial}{\partial z}\left(\frac{1}{r}\frac{\partial WB}{\partial z}\right) = \mu 0 J \quad (1)$$

In which ΨB is the magnetic stream function defined by $\Psi_B(r, z, t) = rA_\varphi(r, z, t)$, where A_φ is the azimuthal component of A and (r, z, t) is the cylindrical coordinates. Also, we have:

$$J = \begin{cases} J_d^{coil} + J_e^{coil} = J0\cos\omega t - \frac{\sigma co}{r}\frac{\partial WB}{\partial t} \\ J_e^{conductor} = -\frac{\sigma c}{r}\frac{\partial WB}{\partial t} \end{cases} \quad (2)$$

where σ_{co} and σ_w are the electrical conductivities of the induction coil and workpiece, respectively. Setting $J_d = J_0\cos\omega t$ as the driving current in the coil we can find a solution of the form

$$\Psi B(r, z, t) = C(r, z)\cos\omega t + S(r, z)\sin\omega t \quad (3)$$

where $C(r, z)$ is the in-phase component and $S(r, z)$ is the out-of-phase component of the solution, ω frequency of the electrical current in the induction coil and t the time. After solving (1) for ΨB, the volumetric power generation in the metallic parts can be calculated via:

$$q(r.z) = \begin{cases} \frac{\sigma co\omega^2}{2r^2}\left[C^2 + \left(\frac{J0r}{\sigma co\omega} - S\right)^2\right] \\ \frac{\sigma c\omega^2}{2r^2}(C^2 + S^2) \end{cases} \quad (4)$$

The boundary conditions are ΨB=0; both in the far-field $(r, z) \to \infty$ and at the axis of symmetry $r = 0$.

2.2. The calculation conditions

The electrical conductivity values used for our calculations are σ_{co}=5.9x10^5 *mho/cm* and σ_w=4x10^4 *mho/cm* and the operating parameters are listed in Table 1. The system under consideration consists of a straight cylindrical conductor (i.e steel workpiece) in the direction of the Oz (i.e., Oz is the centerline) surrounded by a cylindrical induction coil with 6 hollow rectangular copper screws, Fig. 1. The driving current density in the induction coil is calculated by $j_0=(\sigma_{co}V_{coil})/2\pi R_{co}N$, where V_{coil} is the total voltage of the coil, R_{co} is the mean value of the coil radius and N is the number of coil turns. For the magnetic permeability μ, we assume that it is everywhere the constant value of free space (i.e., $\mu_r \approx 1$ where μ_r is the relative magnetic permeability).

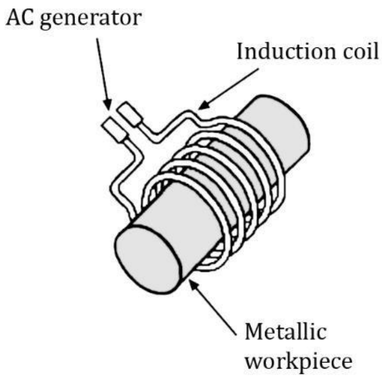

Fig. 1. Basic parts of an induction heating system

It may be mentioned mention that, the skin effect will be found in every metallic workpiece located near the induction coil. This is one of the major factors that causes the eddy current to be concentrated in the surface layer (skin) of the workpiece. Due to this effect, approximately 63% of the eddy current is concentrated in a surface layer of the workpiece. This layer is called the reference depth (or penetration) (δ). The degree of skin impact depends on the frequency and properties of the material (electrical acceptance and relative magnetic permeability) of the conductor [1,2]. Penetration depth is described in meters as [2]

$$\delta = 503\sqrt{\frac{1}{\sigma\mu_r f}} \quad (5)$$

where σ is the electrical conductivity of metal in $(\Omega.m)^{-1}$ and f is the frequency in *Hz* or *cycles/second*. Penetration depth is also a measure of the field penetration depth into the conductors. For the metallic workpiece, four thicknesses are considered: 1, 2, 5, and 25 *mm* and for each thickness, the frequency changes in the range of 1 *kHz* to 100 *kHz*.

2.3. Numerical method

We use the 2D finite element method (FlexPDE package [7]) to numerically solve the involved partial differential equations. After solving the set of paired equations, the distribution and amount of heat-induced in each metal part of the studied system can be obtained.

The computational domain with the non-structural finite element triangle mesh is shown in Fig. 2. In the space close to and in the metal parts, the employed grid must be fine enough to obtain a good quality solution because of the high gradients of the electromagnetic fields. It should be noted that the grid size becomes smaller by increasing the applied frequency which can significantly increase the computation time. It should be carefully done and has to be well controlled to guarantee the accuracy of numerical results at all frequencies.

The results based on this set of parameters will be presented in the following section.

Table 1
Operating parameters used for calculations.

Description (units)	Symbol	Value
Workpiece outer radius (*mm*)	r_w	25
Workpiece thickness (*mm*)	l_w	1,2,5,25
Workpiece height (*mm*)	h_w	93
Coil inner radius (*mm*)	r_{co}	85
Coil width (*mm*)	l_{co}	10
Coil wall thickness (*mm*)	L_{co}	1
Height of coil turns (*mm*)	h_{co}	13
Distance between coil turns (*mm*)	d_{co}	3

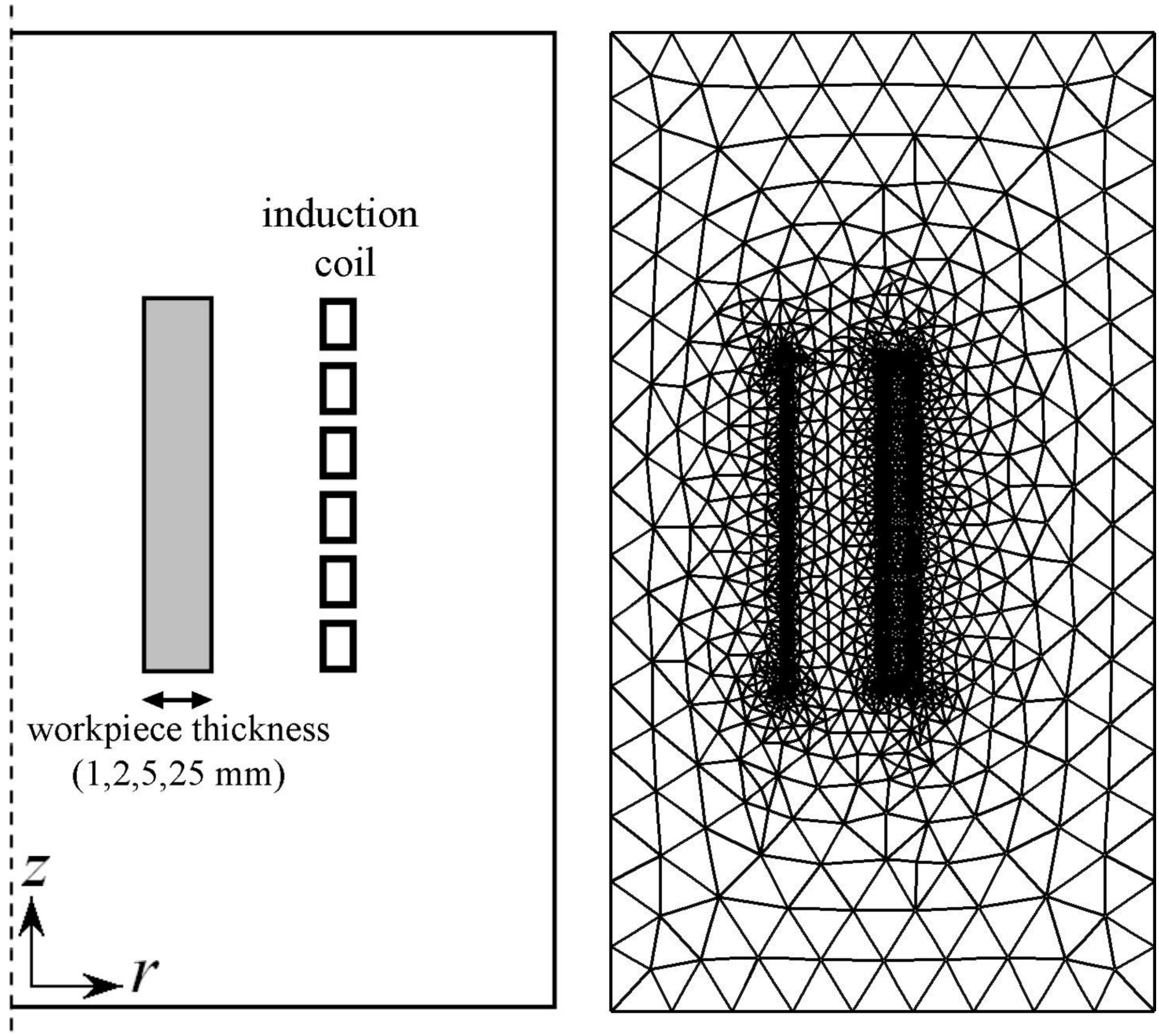

Fig. 2. Sketch of the induction heating setup including a right cylindrical workpiece and a multi turn RF-coil (left) and FEM grid (right)

3.Results and discussion

Figure 3 shows the distributions of an in-phase component and out-of-phase component of the magnetic stream function (Ψ_B) in the heating system for 1 *mm* workpiece thickness and frequency of 1, 10, and 100 *kHz*. For all cases, the maximum of in-phase component (C) is located at the lowest and top edges of the RF-coil but its minimum is located on the middle of the workpiece for low frequencies (f < 5 *kHz*) and then is shifted towards the workpiece ends which is located in that place for high frequencies (f > 10 *kHz*). The intensity of $C_{\max}$ and $|S_{\max}|$ decreases with the increasing of the applied frequency. Also $|S_{\max}/C_{\max}|\sim 1$ for low frequencies while $|S_{\max}/C_{\max}|\sim 3$ and $|S_{\max}/C_{\max}|\sim 2$ for middle and high frequencies, respectively. It is interesting to note that the C-gradient becomes extremely high with raising the applied frequencies.

For the out-of-phase component (S), the maximum is located at the outer surfaces of the induction coil turns and its distribution has an approximately linear gradient in the space between the coil and the workpiece. The workpiece tends to remove electromagnetic field components from its body, causing them to become more intense in the space between the workpiece and the coil than elsewhere. This behavior becomes stronger with increasing frequency, and as a result, the workpiece acts as a shield for this electromagnetic component for the high applied frequencies.

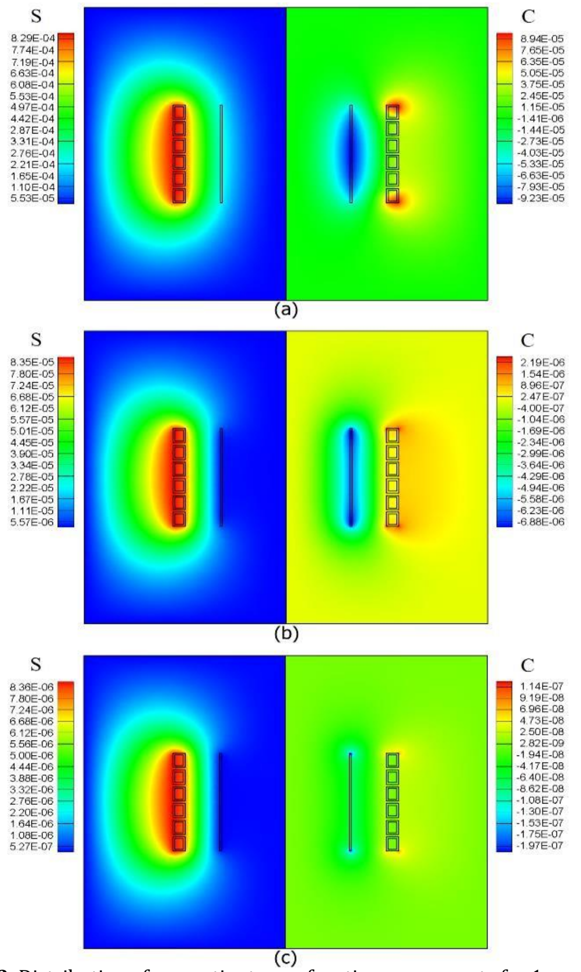

Fig. 3. Distribution of magnetic stream function components for 1 *mm* workpiece thickness (a) f=1 *kHz*, (b) f=10 *kHz*, and (c) f=100 *kHz*

As can be seen, all components decrease by frequency rising, whereas their distribution is changed totally. According to Eq. (4), the distribution and amount of magnetic stream function components have a major role in the determination of heat generation, so it may estimate that input current frequency has a great effect on the induced heat in any part of the induction heating system. In this regard doing so, the distribution of generated energy is calculated for a sample cylindrical workpiece in the frequencies of 1, 10, and 100 *kHz*, Fig. 4. It is obvious that both intensity and distribution of produced heat change when the frequency is changed. For a closer look, we need to look at some other features such as efficiency changes and thermal characteristics along the sidewall surface of the workpiece.

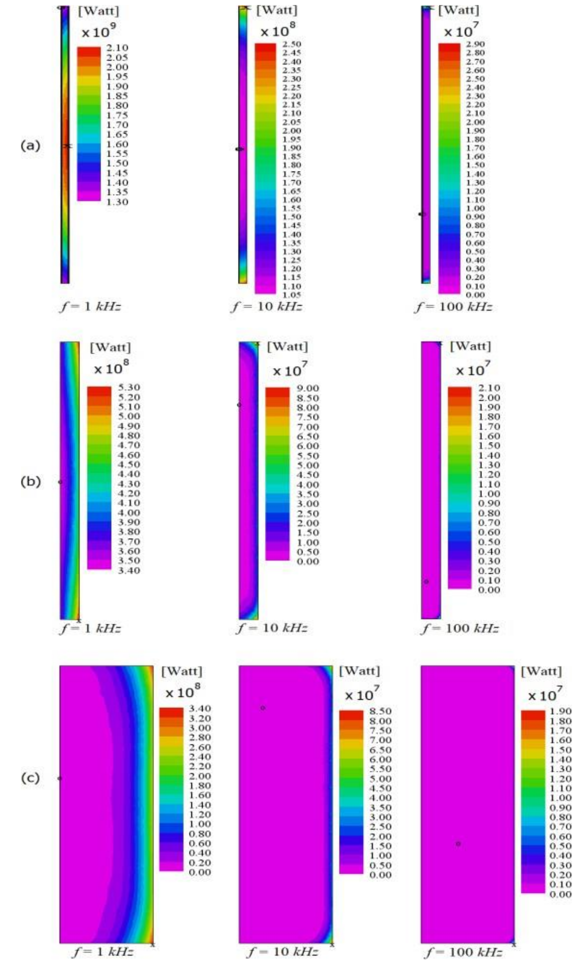

Fig. 4. Distribution of workpiece generated heat for f = 1, 10 and 100 *kHz* in (a) 1 *mm*, (b) 5 *mm* and (c) 25 *mm* workpiece thickness

At first glance, we may suppose that low frequencies must be applied for extra heat generation in the workpiece. But it is necessary to keep in mind that the heat is generated in all metallic parts of the system such as the induction coil. The generated heat in the induction coil is a harmful factor, so usually, a quenching system is applied to remove this heat.

Due to the above points, two frequency ranges are limited for a particular application by:

1. High frequencies in which the generated heat in the workpiece has low intensity for this application.
2. Low frequencies in which the generated heat in the induction coil has high intensity and cooling process can not remove it.

Since only the generated heat in workpiece is useful, the efficiency of induction heating process can be defined as:

$$\text{Efficiency} = \frac{\text{Amout of generated heat in workpiece}}{\text{Amout of generated heat in all metallic parts}} \quad (6)$$

Figure 5, shows the variation of efficiency vs. frequency. For 1 *mm* workpiece thickness, when the frequency increased over 1 *kHz*, the efficiency of the process will increase and at 5250 *Hz*, the efficiency will reach a peak. When the frequency increased more than 5250 *Hz*, the efficiency will decline.

For 2 *mm* thickness, the efficiency graph is basically similar to the 1 mm workpiece graph, but the maximum is observed at 3650 *Hz*.

For 5 and 25 *mm* thicknesses, the efficiency will increase by the frequency rising in the range of 1-11 *kHz* then has negligible changes in higher frequencies. Also, it is estimated that the maximum efficiency is greater for thin workpieces, as the maximum efficiency for 1 *mm* workpiece is 80.6% and for 2 *mm* one is 71.2%. But for two other workpieces in most frequencies, the efficiency is almost stable. For 5 *mm* workpiece in the frequency range of 1-100 *kHz*, the efficiency changes from 52.2% to 57.4%, and for 25 *mm* workpiece the efficiency changes from 50.3% to 57% in the frequency range of 3-100 *kHz*.

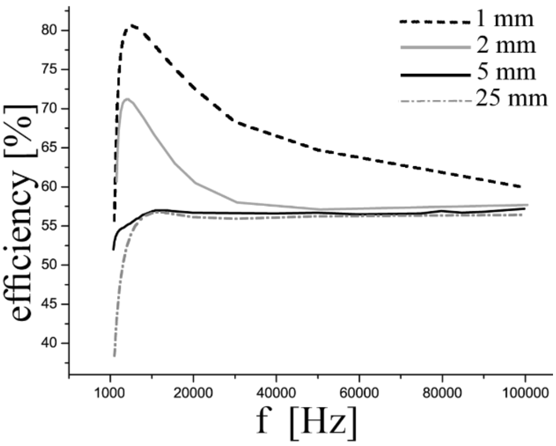

Fig. 5. Changes of induction heating process efficiency in terms of input current frequency

The heat distribution on the outer surface of the workpiece wall is another crucial subject in heat treatment applications. Fig. 6, shows the heat distribution on the outer surface wall of 1, 2, and 5 *mm* workpiece for 4 different frequencies. As can be seen, the heat generation is at its maximum value at the middle portion of the outer surface of the workpiece wall in frequencies less than 3700 *Hz*. But in frequencies above 3700 *Hz*, this hot spot is shifted to the corners of the outer surface of the workpiece wall. This is because in low frequencies, the current penetration depth is great and the system has a good coupling. Therefore, there will be intense heating due to the Joule effect. As a result, the heat pattern will be relatively narrow and deep. Therefore, the maximum heat point will be in the middle of the outer surface of the workpiece wall. At high frequencies, the system has a weak coupling and the heat pattern will be much wider and shallow, so the electric field can penetrate from both ends of the workpiece, and the maximum heat point is transmitted to these endpoints. [2]. In frequencies about 3700 *Hz*, the heat distribution on the outer wall of the workpiece is almost uniform, so these frequencies can be used in applications in which uniform heat distribution is needed. It is also observed that as the thickness of the workpiece increases, the frequency of almost uniform heat production at the outer surface of the workpiece wall decreases, as in 2 *mm* workpiece the 1.8 *kHz* and in 5 *mm* workpiece the 800 *Hz* will produce an almost uniform heat distribution on the outer surface of workpiece wall.

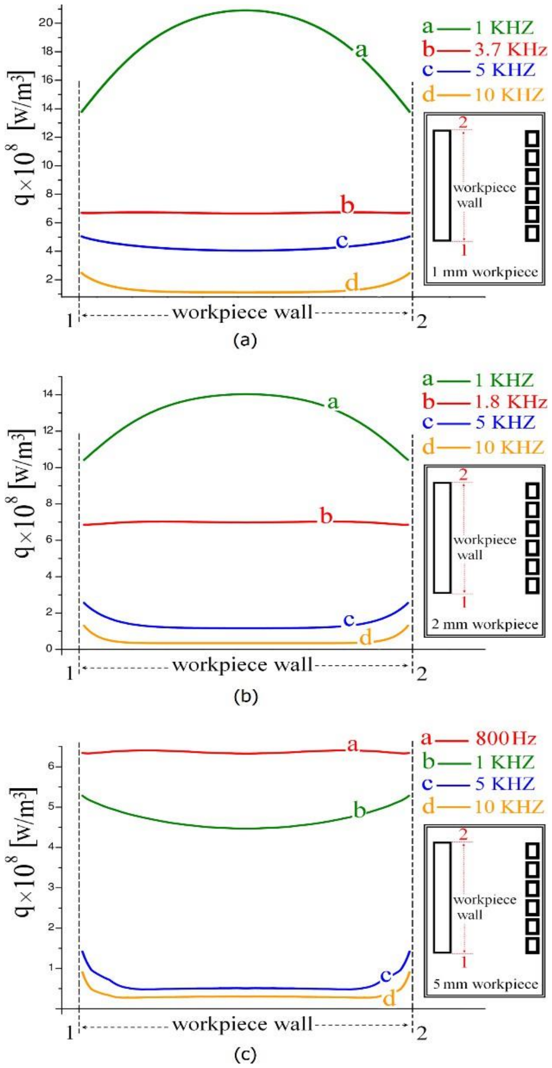

Fig. 6. Changes of heating patterns in the outer surface of workpiece wall in terms of input current frequency for, (a) 1 *mm*, (b) 2 *mm*, and (c) 5 *mm* workpiece thickness

4. Conclusions

To study the effect of input current frequency on the heat generated in the workpiece and induction coil, a series of numerical calculations were performed. It can be concluded from the obtained results:

1. In determining the appropriate frequency for a particular application, the most important

parameter is the amount of heat production required in the workpiece. The results show that for all thicknesses of the workpiece, the amount of heat produced in the workpiece decreases with increasing frequency.

2. Another important parameter is the amount of heat produced in the induction coil, which is a harmful factor. Similar to the previous point, the amount of energy produced in the induction coil decreases with increasing frequency. Of course, the heat generated is equal for all thicknesses of the workpiece. This means that the heat is independent of the thickness of the workpiece.
3. Frequency changes can shift the location of the maximum heat point generated on the outer surface of the workpiece wall. At low frequencies, the maximum heat is placed in the middle of the outer surface of the workpiece wall, and as the frequency increases, the maximum point is transferred to the two corners of the outer surface of the workpiece wall. In another word, by frequency increasing, the heating patterns become wider and shallower. Also, by selecting a specific frequency that depends on the thickness of the workpiece, a uniform heat distribution can be created on the outer wall. This specific frequency decreases with the increasing thickness of the workpiece.

References

[1] A.F. Leatherman, D.E. Stutz, Induction heating advances, National Aeronautics and Space Administration, 1969.

[2] V. Rudnev, D. Loveles, R. Cook, M. Black, Handbook of induction heating, New York NY. 2003.

[3] E. Rapoport, Y. Pleshivtseva, Optimal control of induction heating processess: Taylor & Francis Group, LLC. 2006.

[4] J.D. Lavers, State of the art of numerical modeling for induction processes, COMPEL, 27 (2008) 335-349.

[5] M.H. Tavakoli, H. Karbaschi, F. Samavat, Computational modeling of induction heating process, Progress in Electromagnetics Research Letters, 11 (2009) 93-102.

[6] M.H. Tavakoli, H. Karbaschi, F. Samavat, Computational Study of Electromagnetic Fields, Eddy Currents and Induction Heating in Thin and Thick Workpieces, Commun. Comput. Phys, 8 (2010) 211-225.

[7] https://www.pdesolutions.com.